Physical Review & Research International
3(4): 556-567, 2013

SCIENCEDOMAIN *international*
www.sciencedomain.org

Effect of Diurnal Changes on the Quality of Digital Images

Priti Rajput[1], Santoresh Kumari[2], Sandeep Arya[3] and Parveen Lehana[3*]

[1]Directorate of Economics and Statistics, J & K, India.
[2]Department of Computer Science, MIET Jammu, J & K, India.
[3]Department of Physics and Electronics, University of Jammu, Jammu, J & K, India.

Authors' contributions

This work was carried out in collaboration between all authors. All authors read and approved the final manuscript.

Research Article

Received 7th May 2013
Accepted 17th July 2013
Published 23rd July 2013

ABSTRACT

Prospective outdoor imaging depends on diurnal changes through the day and it needs an understanding of light and its effects on quality of the images. In this paper, investigations have been carried out to study the effect of diurnal changes on the quality of the images taken at regular intervals of one hour from sunrise to sunset in a sunny day. For investigating the effect of sun orientation, the images were also taken in four different directions i.e. East, West, North, and South. The analysis of the results showed that the picture quality varies with respect to time and the orientation.

Keywords: Digital image processing; diurnal change; image quality; image analysis.

1. INTRODUCTION

Digital image processing has several significant applications in the field of weather forecasting, medical resonance imaging, computed tomography, cryptography, and astronomy as well as in other areas of research and technology [1-5]. Generally, image

[*]Corresponding author: Email: pklehana@gmail.com;

processing is used to extract some valuable features of an image like visualization, image sharpening and restoration, image retrieval, pattern measurements, image recognition, and many more [6-11]. Digital image processing involves a series of complex parameters that help to acquire the better digital image [12]. In image processing, the effect of light relates the “hardness” or “softness” of the image. This effect is perceptible in overcast weather conditions. The sun-drenched light up the whole ambience and creates liveliness in the images. An intense point source may badly affect the images. The change in the direction of light also affects the images.

The exact color of lighting in the images taken can be measured as “color temperature”. The units are degree Kelvin [13]. Interestingly, the lower temperature implies warmer color tones (red and yellows) while the higher temperature create cooler colors (blues). Throughout the day, the color temperature of lighting conditions outside changes constantly. It’s quite interesting that the color of the lighting conditions changes throughout the day due to position of the sun and the properties of the atmosphere. Air scatters blue light more strongly than the red light. Before sunrise, the sun is stumpy and the illumination floats horizontally across the landscape, thus the illumination comes indirectly from the air that creates a typical blue color [2,14]. As the sun rises, light penetrates through the thick layers of atmosphere and filters out the blue light, thus giving a warm red color. Similarly, after the sunset, the lighting conditions suddenly become intense blue in shade [2,13]. Overhead sun at noon produces neutral colours, though it will not produce a good quality image. The colour temperature in shade on a sunny day is extremely high as all of the lighting comes from the blue sky. In afternoon, the colour temperature falls as the sun goes down and the effect become warmer and redder [14]. During cloudy days, the change in colours is much perceptible due to filtering of light in clouds resulting in neutral light throughout the day [14,15].

In this paper, we have investigated the effect of diurnal changes and orientation of the sun on the quality of the open-air natural images. The mathematical formulations of the quality of digital images are presented in the following section. The methodology adopted for the investigations is discussed in Section 3. The results and discussions are presented in Section 4.

2. MATHEMATICAL FORMULATION

Although visual perception plays a vital role in assessing the quality of a digital image, automatic assessment using objective measures is some time useful for the comparison. One method for this assessment from [16-18] is described here. It uses contrast (σ_n), intensity (μ_n), sharpness (*s*) in normalized form for estimating the quality of the given image [19-22].

2.1 Normalized Intensity Parameter

Let μ_n be the normalized intensity parameter, then, for grey scale images, normalized intensity parameter can be evaluated as

$$\mu_n = \begin{cases} \dfrac{\mu}{255} & \text{for } \mu < 154 \\ 1 - \dfrac{\mu}{255} & \text{otherwise} \end{cases} \quad (1)$$

where μ is the mean contrast of the image. A region is considered to have adequate intensity for 0.4 ≤ μ_n ≤ 0.6 [21,22].

2.2 Normalized Contrast Parameter

The normalized contrast parameter (σ_n) can be given as

$$\sigma_n = \begin{cases} \dfrac{\sigma}{128} & \text{for } \sigma \le 64 \\ 1 - \dfrac{\sigma}{128} & \text{otherwise} \end{cases} \quad (2)$$

where σ is the standard deviation. A region is considered to have enough contrast when 0.25 ≤ σ_n ≤ 0.5. For, σ_n < 0.25, the region has poor contrast and σ_n > 0.5, the region has too much contrast [21] [22].

2.3 Normalized Sharpness Parameter

Sharpness (*s*) is directly proportional to the high frequency content of an image and is given as,

$$s = \sqrt{\| h \otimes I \|}^2 = \sqrt{\sum_{\upsilon_1=0}^{M_1-1} \sum_{\upsilon_2=0}^{M_2-1} \left| \hat{h}[\upsilon_1, \upsilon_2] \hat{I}[\upsilon_1, \upsilon_2] \right|} \quad (3)$$

where h is a high pass filter obtained from the inverse discrete Fourier transform (IDFT) and $\hat{h}$ is its direct Discrete Fourier Transform (DFT) . $\hat{I}$ is the DFT of Image I . The role of $\hat{h}$ (or h) is to weight the energy at the high frequencies relative to the low frequencies, thereby emphasizing the contribution of the high frequencies to *s*. The larger the value of *s*, greater is the sharpness of I .

Conversely,

$$h = \text{IDFT}\left(1 - exp\left(-\frac{v_1^2 + v_2^2}{\alpha^2}\right)\right) \quad (4)$$

where v_1 and v_2 are the spatial parameters. Here, α is the attenuation parameter representing decaying of the impulse response of the Guassian filter. A smaller value of α implies that fewer frequencies are attenuated and vice versa. The parameter I represents the given image [21,22].

2.4 Image Quality Factor

The parameters σ_n, μ_n, and *s* are used for evaluating the image quality or quality factor (Q) defined as

$$Q = 0.5\mu_n + \sigma_n + 0.1s \tag{5}$$

where the value of Q lies between 0 and 1. When Q > 0.55, the quality is considered to be good and is poor for Q <= 0.5. The quality of an image expresses the hidden details in the image. An image is considered as good only if the good regions in the image are more than 60% [15].

3. METHODOLOGY

The lighting conditions from dawn to dusk and the orientation of the sun with respect to the image affect the quality of the captured images. The quality assessment of digital images in an open-air environment under the impact of natural light (non -uniform source of energy) is little complicated. For investigating the effect of diurnal changes and orientation, the images were taken with a 9.1 mega pixel digital camera after regular intervals of 1 hour from sunrise to sunset under the clear vision of natural light. Simultaneously, the images were also taken from four different directions (East, West, North, and South).

The steps involved for the investigations are shown in Fig. 1. The images were resized and 100 sub images (each of size 10×10 pixels) were constructed. To reduce the bias, each sub image was constructed by selecting 100 random pixels from the given image. The quality factor for each sub image was estimated. On the basis of preliminary investigations it was found that equation (5) may be slightly modified by attaching a weighting factor of 0.6 to the normalized contrast (σ_n). The overall quality of the image was estimated by taking the mean of all the quality factors. One set of four images taken early morning is shown in Fig. 2 to Fig. 5. The same set of images was taken after regular time intervals of 1 hour till the time of sunset on 22nd March, 2013 at Jammu. A total of 13 sets were from 6:50 am to 6:50 pm. These images were resized to 512 x 512 pixels. The effect of diurnal changes was observed for each primary color (color red, green, and blue) and grey scale image.

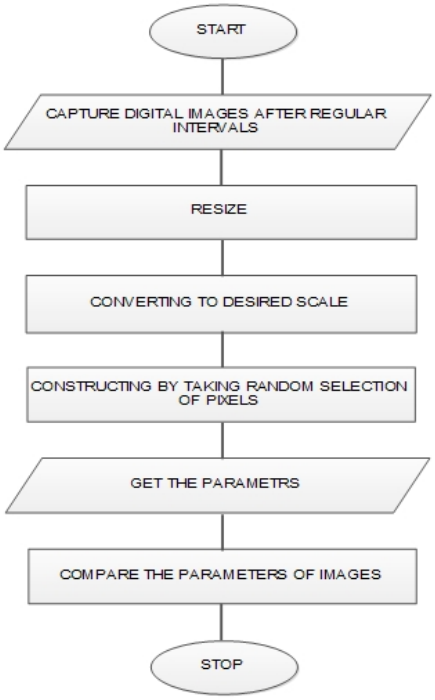

Fig. 1. Steps used for the investigations

Fig. 2. Image taken in East direction

Fig. 3. Image taken in West direction

Fig. 4. Image taken in North direction

Fig. 5. Image taken in South direction

4. RESULTS AND DISCUSSIONS

The analysis of the quality of images was carried out with respect to time and orientation. The images were taken with a single camera; however a three legged stand was used for capturing the images. The camera was tightly attached to the stand so that image should be captured at the same angle. Only one camera was used and at one time in one direction only one image was taken. For convenience, the results are presented under the following four sub sections.

4.1 Analysis with Respect to East

The estimated means and the standard deviations of sub images in East direction are listed in Table 1 and plotted in Fig. 6. All the components images for Red, Green, Blue, and Grey show a high quality image at around 12:50 and poor quality image at 18:50 except for the non-clear blue at 6:50. The average value for the quality of images stands at 0.43, 0.44, 0.45, and 0.44 for red, green, blue, and grey images, respectively.

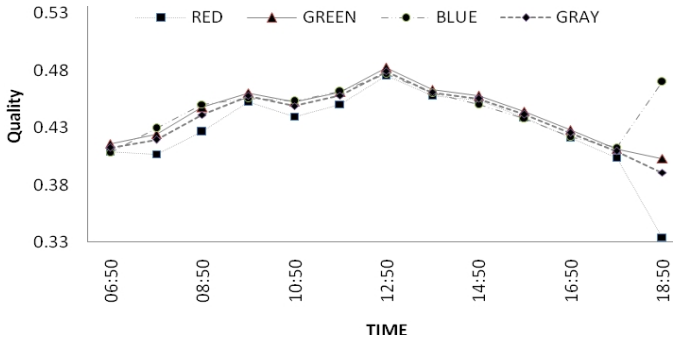

Fig. 6. Quality versus time plot in East

Table 1. Mean quality and standard (SD) deviation in East

Time	Red		Green		Blue		Gray	
	Mean	SD	Mean	SD	Mean	SD	Mean	SD
06:50	0.409	0.004	0.416	0.004	0.408	0.004	0.413	0.003
07:50	0.407	0.003	0.425	0.003	0.429	0.004	0.420	0.003
08:50	0.426	0.002	0.448	0.002	0.450	0.003	0.442	0.002
09:50	0.453	0.003	0.460	0.004	0.456	0.003	0.458	0.003
10:50	0.440	0.002	0.453	0.002	0.453	0.003	0.449	0.002
11:50	0.450	0.002	0.461	0.002	0.462	0.003	0.458	0.003
12:50	0.476	0.003	0.482	0.003	0.477	0.003	0.479	0.003
13:50	0.458	0.002	0.463	0.003	0.460	0.003	0.461`	0.002
14:50	0.454	0.002	0.458	0.002	0.450	0.003	0.455	0.002
15:50	0.439	0.002	0.444	0.002	0.438	0.003	0.442	0.002
16:50	0.421	0.002	0.428	0.002	0.422	0.003	0.426	0.002
17:50	0.404	0.002	0.412	0.002	0.413	0.003	0.410	0.002
18:50	0.334	0.002	0.403	0.002	0.470	0.003	0.391	0.002

4.2 Analysis with Respect to West

The estimated means and the standard deviations of sub images in West direction are listed in Table 2 and plotted in Fig. 7. The quality of images falls from 6:50 to 7:50 for all colours and shows an irregular pattern till 10:00. The high quality images were obtained around 13:50 for red and grey whereas for green and blue at 15:50. Except for the blue, the poor quality images are obtained around 9:50. The average value of quality comes around 0.43, 0.45, 0.45, and 0.45 for red, green, blue, and grey component, respectively. The average value for all the components stands around 0.44. The highest quality image is obtained for blue at around 13:50. Among all the four colors, the blue component shows good results followed by green, grey, and red.

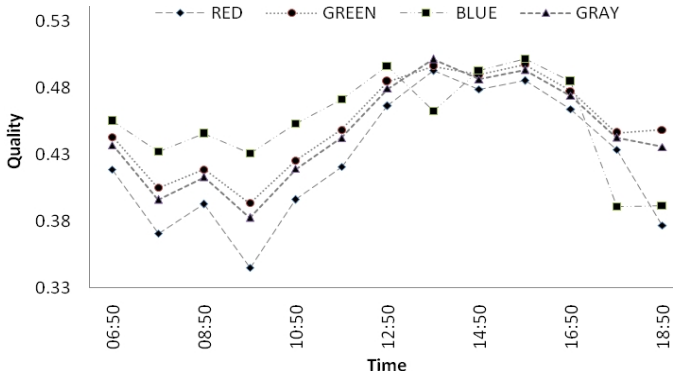

Fig. 7. Quality versus time plot in West

Table 2. Mean quality and standard deviation (SD) in West

Time	Red		Green		Blue		Gray	
	Mean	SD	Mean	SD	Mean	SD	Mean	SD
06:50	0.419	0.003	0.443	0.003	0.455	0.003	0.437	0.002
07:50	0.371	0.002	0.405	0.002	0.432	0.003	0.396	0.002
08:50	0.393	0.002	0.419	0.002	0.445	0.003	0.413	0.002
09:50	0.345	0.001	0.393	0.002	0.431	0.002	0.383	0.002
10:50	0.396	0.002	0.426	0.002	0.453	0.003	0.419	0.002
11:50	0.421	0.002	0.448	0.003	0.472	0.003	0.442	0.003
12:50	0.466	0.003	0.485	0.003	0.497	0.003	0.479	0.003
13:50	0.493	0.003	0.496	0.029	0.463	0.052	0.501`	0.003
14:50	0.479	0.003	0.490	0.004	0.493	0.004	0.486	0.003
15:50	0.485	0.003	0.498	0.003	0.502	0.003	0.493	0.003
16:50	0.464	0.003	0.478	0.003	0.485	0.003	0.474	0.003
17:50	0.433	0.003	0.446	0.003	0.391	0.003	0.443	0.003
18:50	0.377	0.002	0.449	0.003	0.392	0.003	0.436	0.002

4.3 Analysis with Respect to North

Mean and the standard deviation of the quality factors of sub images for North direction are listed in Table 3 and plotted in Fig. 8. The quality is better around 8:50 and poor at 18:50.

Red component becomes more prominent after sunrise. This effect neutralizes as the sun moves to noon. The quality of image deteriorates after noon and reaches to a minimum value after sunset. For red component, the average value of the quality of image lies around 0.43. For green component, the quality of image is highest around 8:50 and lowest around 17:50. The average value lies around 0.44. In comparison to red, quality of green component is relatively better. The minimum value of quality for red falls to 0.36 where as it stays around 0.40 for green. The effect on the quality for blue is more pronounced for all images as compared to the other components. The highest value is observed at 18:50 and the lowest at around 17:50. The average value lies around 0.44. After sunset the light in atmosphere shifts to blue and thus the quality of images shoots up. For grey-scale, good quality image is obtained at around 8:50 and the quality deteriorates to the minimum value around 18:50 though the average value sustains at 0.43. The quality curves of grey and green show almost similar pattern. The maximum and min value for the two are almost the same. The quality of images from 6:50 to 8:50 does not show any strong variation for any of the color component. The best quality is obtained at around 8:50 in the morning for all the colors except blue for which the highest quality is obtained at 18:50 due to the fact that the sky scatters more blue light just after sunset. The red and green component shows a reverse behavior at 18:50, the blue shows a high quality image whereas the red one shows a poor quality image. Of all the four components, the average quality of blue remains slightly better.

Table 3. Mean quality and standard deviation (SD) in North

Time	Red		Green		Blue		Gray	
	Mean	SD	Mean	SD	Mean	SD	Mean	SD
06:50	0.410	0.003	0.425	0.003	0.425	0.004	0.420	0.003
07:50	0.412	0.003	0.423	0.003	0.424	0.003	0.419	0.003
08:50	0.462	0.002	0.474	0.002	0.469	0.003	0.470	0.002
09:50	0.420	0.002	0.440	0.002	0.452	0.003	0.436	0.002
10:50	0.449	0.002	0.451	0.002	0.445	0.002	0.450	0.002
11:50	0.432	0.002	0.451	0.002	0.455	0.002	0.447	0.002
12:50	0.455	0.002	0.457	0.003	0.444	0.002	0.455	0.003
13:50	0.443	0.002	0.444	0.002	0.436	0.003	0.443	0.003
14:50	0.425	0.003	0.432	0.003	0.427	0.003	0.429	0.003
15:50	0.430	0.003	0.432	0.003	0.425	0.003	0.431	0.003
16:50	0.427	0.003	0.432	0.003	0.424	0.003	0.429	0.003
17:50	0.403	0.002	0.410	0.002	0.412	0.003	0.408	0.002
18:50	0.361	0.002	0.417	0.003	0.476	0.003	0.407	0.003

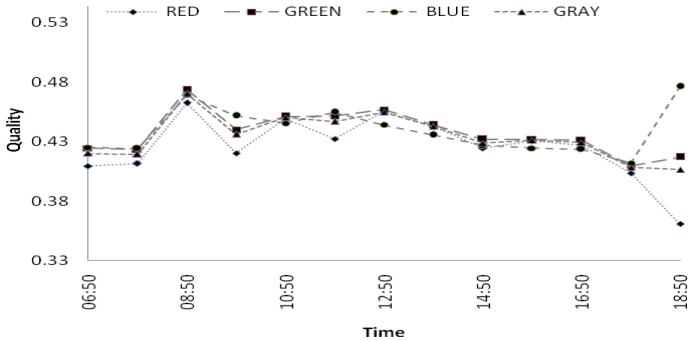

Fig. 8. Quality versus time plot in North

4.4 Analysis with Respect to South

Mean and the standard deviation of quality factors of sub images for South are listed in Table 4 and plotted in Fig. 9. The quality of image for red component is highest around 13:50 and poorest around 18:50. The average quality of image lies around 0.44. The quality factor for red increases as the sun rises and attains its maximum value around 13:50 and thereafter a decrease in quality is noticed. Before sunset, the quality of red images shows a slight improvement as compared to other component colors. After sunset, the quality falls to a minimum value. The effect of green and grey components is almost same. The high quality image is obtained around 13:50 and poor quality around18:50. The average quality for grey and green is around 0.45. The effect of on blue is slightly more than other components. The highest quality is obtained at 18:50 and poorest at 17:50. The average quality lies around 0.45. For all the components, high quality image is obtained for blue and poor for red.

Table 4. Mean quality and standard deviation (SD) in South

Time	Red		Green		Blue		Gray	
	Mean	SD	Mean	SD	Mean	SD	Mean	SD
06:50	0.413	0.004	0.430	0.003	0.429	0.003	0.425	0.003
07:50	0.430	0.002	0.449	0.003	0.448	0.004	0.443	0.004
08:50	0.446	0.003	0.459	0.003	0.460	0.003	0.455	0.003
09:50	0.446	0.003	0.464	0.004	0.461	0.004	0.458	0.004
10:50	0.455	0.004	0.462	0.004	0.451	0.003	0.458	0.003
11:50	0.433	0.003	0.445	0.003	0.441	0.004	0.441	0.003
12:50	0.442	0.003	0.452	0.003	0.446	0.004	0.449	0.003
13:50	0.472	0.003	0.472	0.003	0.455	0.003	0.470`	0.003
14:50	0.449	0.003	0.453	0.003	0.436	0.003	0.450	0.003
15:50	0.455	0.002	0.458	0.003	0.443	0.003	0.455	0.003
16:50	0.441	0.003	0.442	0.003	0.429	0.002	0.440	0.003
17:50	0.451	0.002	0.446	0.003	0.429	0.003	0.445	0.002
18:50	0.348	0.002	0.412	0.003	0.479	0.003	0.400	0.002

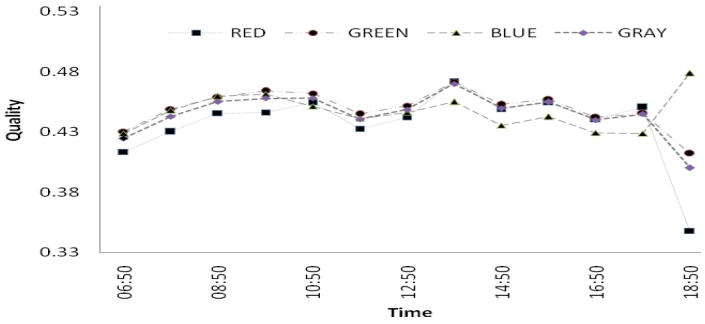

Fig. 9. Quality versus time plot in South

The quality for different components is plotted in Fig. 10 to Fig. 13. The quality of red images is highest in West direction at 13:50 and lowest in East at 18:50. The average value of red component stands at 0.43, 0.43, 0.43, 0.44 for East, West, North, and South, respectively. The average quality for green is around 0.44, 0.45, 0.44, 0.45, for East, West, North, and

South, respectively. The quality of blue is high in West around 15:50 and lowest in West around 17:50. The average quality of blue is 0.45, 0.45, 0.44, 0.45 in East, West, North, and South, respectively. It is highest and lowest in West around 13:50, and 9:50, respectively. The average quality for grey is around 0.44, 0.45, 0.43, 0.45, in East, West, North, and South, respectively.

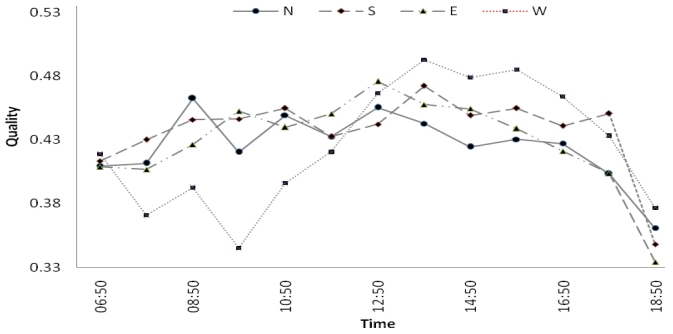

Fig. 10. Quality versus time plot for red

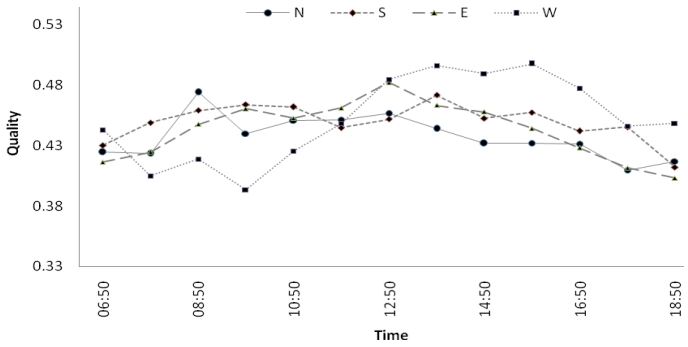

Fig. 11. Quality versus time plot for green

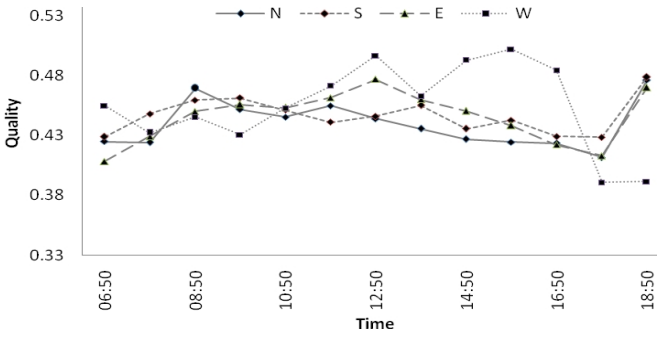

Fig. 12. Quality versus time plot for blue

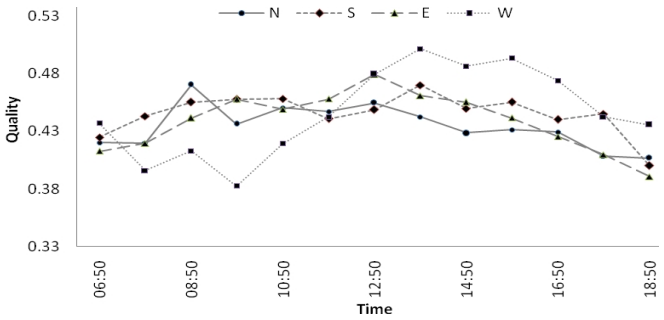

Fig. 13. Quality versus time plot for grey

5. CONCLUSION

Analysis has shown that the behavior of red, green, blue, and grey component is the same in all directions except for the blue in West direction. The blue component provides good quality at 18:50 except in West direction. It has been observed that West orientation has considerable effect on the quality of the images. Hence, experienced photographers try to align their camera along this direction for quality imaging.

The investigations were carried out to examine the effect of diurnal changes and orientation of sun on the objective quality of the digital images. The images were taken at regular time intervals of one hour in four directions. Images were little blurred and noisy during the sunrise and sunset. Comparison of objective and subjective quality is on the plan for future work.

COMPETING INTERESTS

Authors have declared that no competing interests exist.

REFERENCES

1. Gonzalez R, Woods R. Digital Image Processing. 2nd edition, Prentice Hall; 2002.
2. Kensek K, Suk JY. Daylight Factor (overcast sky) versus Daylight Availability (clear sky) in Computer-based Daylighting Simulations. Journal of Creative Sustainable Architecture & Built Environment. 2011;1:3-14.
3. Arya S, Khan S, Kumar D, Dutta M, Lehana P. Image enhancement technique on Ultrasound Images using Aura Transformation. International Journal in Foundations of Computer Science & Technology. 2012;2(3):1-10.
4. Arya S, P Lehana. Development of seed analyzer using the techniques of computer vision. International Journal of Distributed and Parallel Systems.2012;3(1):149-155.
5. Lehana P, Devi S, Singh S, Abrol P, Khan S, Arya S. Investigations of the MRI Images using Aura Transformation. Signal & Image Processing: An International Journal. 2012;3(1): 95-104.
6. Ito M. Extraction of fine blood vessels from an ultrasound image by adaptive local image processing. International Journal of Modelling, Identification and Control. 2008;4:331-336.

7. Zhang H, Zhao W, Ren D, Qu Y. Laser linewidth measurement based on image processing and non-air gap F-P etalon," in Proc. of International Symposium on Photoelectronic Detection and Imaging. 2009;7384..
8. Rodriguez P, López-de-Teruel A, Ruiz G. Garcia-Mateos, L. Farnandes. Q Vision. A development framework for real-time computer vision and image processing research, in Proc. International Conference on Image Processing, Computer Vision, & Pattern Recognition. 2008;2.
9. Xu Z, Li S, Yoon S, Toumi K, Burns D. Complete surface distinguishing and overlapping technology for three-dimensional image processing of micro devices, in Proc. 5th International Symposium of Nanomanufacturing, Singapore; 2008.
10. Xiao Z, Guo G, Wang X. A study of optical system and image processing in Vickers hardness photoelectric detection system, in Proc. International Conference on Optical Instruments and Technology: Optoelectronic Imaging and Process Technology. 2009; 7513.
11. Mavi M Kaur. Identify Defects in Plastic (gears) using Digital Image Processing- A Review, International Journal of Computer Science and Information Technology & Security. 2012;2:342-344.
12. Thavot R, Mosqueron R, Alisafaee M, Lucarz C, Mattavelli M J, Dubois V. Noel, Dataflow design of a co-processor architecture for image processing," in Proc. Conference on Design and Architectures for Signal and Image Processing; 2008.
13. Wang F, Wang S. Characterization on pore size of honeycomb-patterned micro-porous PET fibers using image processing techniques, Industria Textila. 2010;61:66-69.
14. Gachet P, Geiser F, Laloui L, Vulliet L. Automated digital image processing for volume change measurement in triaxial cells. Geotechnical Testing Journal. 2007;30:98-103.
15. Brunelli R, Poggio T. Face Recognition: Features Versus Templates, IEEE Trans. Pattern Anal. Mach. Intell. 1993;15:1042-1052.
16. Baron RJ. Mechanics of human facial recognition. International Journal of Man Machine Studies. 1981;15:137-138.
17. Jensen J. Introductory digital image processing: A remote sensing perspective," 3rd Edition. Pearson Prentice Hall; 2005.
18. Umbaugh SE. Computer graphics & image processing," *Prentice Hall PTR*, 1998.
19. *Preston Barrows,* "Lighting Conditions from the Sun and Sky Will Change Throughout the Day," http:/voices .yahoo.com/the-color-temperature-lighting –conditions-through the day.
20. Lacewell CW, Gebril M, Buaba R, Homaifar A. Optimization of Image Fusion using Genetic Algorithms and Discrete Wavelet Transform," in Proc. Aerospace and Electronics Conference. 2010;116-121.
21. Erkanli S, Li J, Oguslu E. Fusion of Visual and Thermal Images using Genetic Algorithms ", Bio Inspired Computational Algorithims and their Applications. 187-212. Avaiolable: www.intenchopen.com.
22. Rahman Z. The Lectures Notes of Image Processing, Old Dominion University; 2009.

Peer-review history:
The peer review history for this paper can be accessed here:
http://www.sciencedomain.org/review-history.php?iid=224&id=4&aid=1723